View metadata, citation and similar papers at core.ac.uk

brought to you by CORE

provided by Loughborough University Institutional Repository

A review: microstructure and properties of tin-silver-copper lead-free solder series for the applications of electronics

Muhammad Aamir
School of Engineering, Edith Cowan University, Joondalup, Australia
Riaz Muhammad
Department of Mechanical Engineering, University of Bahrain, Sakheer, Bahrain
Majid Tolouei-Rad
School of Engineering, Edith Cowan University, Joondalup, Australia
Khaled Giasin
School of Mechanical and Design Engineering, University of Portsmouth, Portsmouth, UK, and
Vadim V. Silberschmidt
Wolfson School of Mechanical, Electrical and Manufacturing Engineering, Loughborough University, Loughborough, UK

Abstract

Purpose – The research on lead-free solder alloys has increased in past decades due to awareness of the environmental impact of lead contents in soldering alloys. This has led to the introduction and development of different grades of lead-free solder alloys in the global market. Tin-silver-copper is a lead-free alloy which has been acknowledged by different consortia as a good alternative to conventional tin-lead alloy. The purpose of this paper is to provide comprehensive knowledge about the tin-silver-copper series.

Design/methodology/approach – The approach of this study reviews the microstructure and some other properties of tin-silver-copper series after the addition of indium, titanium, iron, zinc, zirconium, bismuth, nickel, antimony, gallium, aluminium, cerium, lanthanum, yttrium, erbium, praseodymium, neodymium, ytterbium, nanoparticles of nickel, cobalt, silicon carbide, aluminium oxide, zinc oxide, titanium dioxide, cerium oxide, zirconium oxide and titanium diboride, as well as carbon nanotubes, nickel-coated carbon nanotubes, single-walled carbon nanotubes and graphene-nano-sheets.

Findings – The current paper presents a comprehensive review of the tin-silver-copper solder series with possible solutions for improving their microstructure, melting point, mechanical properties and wettability through the addition of different elements/nanoparticles and other materials.

Originality/value – This paper summarises the useful findings of the tin-silver-copper series comprehensively. This information will assist in future work for the design and development of novel lead-free solder alloys.

Keywords Wettability, Alloying element, Mechanical properties, Melting point, Microstructure, Tin-silver-copper series

Paper type Research paper

1. Introduction

Soldering is the joining of two or more metals by means of a third metal, or alloy, with a relatively lower melting point (MP) (Efzan and Marini, 2012). Solder joints are used to physically hold assemblies together, allowing contraction and expansion of different components, dissipating any generated heat and transmitting electrical signals. Therefore, the reliability of a solder joint depends on the performance and quality of the solder alloy (Aamir *et al.*, 2015). In the early era of the microelectronics industry, tin-lead (Sn_{63}-Pb_{37}) was most commonly used (Ma and Suhling, 2009). This was due to the combined merit of low cost and good mechanical, metallurgical and physical properties, mainly facilitated by the lead *(Pb)* (Lee, 1997). However, lead's use in electronics is now restricted by legislation worldwide due to environmental concerns (Cheng *et al.*, 2017). Therefore, electronics manufacturers require a reliable lead-free solder *(LFS)* that is environmentally benign (Lee, 1997).

The most popular *LFS* alloys are in the tin-silver-copper (*SAC*) series (Aamir *et al.*, 2017a; Aamir *et al.*, 2017b). A survey has shown that almost 70 per cent of accepted lead-free solders *(LFSs)* are *SAC* alloys, due to their comparatively good properties (Shnawah *et al.*, 2012). In addition, the *SAC* series provides better mechanical support in electronic devices because of its good joint strength (Harrison *et al.*, 2001). In

SAC, the near eutectic composition consists of a high volume of a β-tin *(Sn)* matrix and intermetallic compounds, *(IMCs)* namely Ag_3Sn, Cu_6Sn_5 and Cu_3Sn (El-Daly *et al.*, 2013). In comparison to the *Sn*-matrix, the *IMCs* are brittle in nature (Sadiq *et al.*, 2013). It is worth noting that the formation of Ag_3Sn is due to the reaction between *Sn* and Silver *(Ag)*, whereas Cu_6Sn_5 is possibly formed by the reaction between *Sn* and copper *(Cu)*. No reaction has been found between *Ag* and *Cu* for the formation of any types of *IMCs* (Vianco and Shangguan, 2006). It has also been reported that Cu_3Sn does not form at the eutectic point unless the content of *Cu* is high enough for its formation at high temperature (Ma and Suhling, 2009). *Cu* additions in the *SAC* series improve their wettability and lower their melting temperature (Nimmo, 2004). Furthermore, higher *Ag* contents in the *Sn*-rich matrix yield a higher amount of Ag_3Sn, which may result in higher strength. However, high *Ag* contents with high elastic moduli *(E)* and yield strengths *(YS)* show reasonably low ductility (Che *et al.*, 2010).

Unfortunately, *SAC* solders still exhibit some problems such as higher *MP*, poor wettability and coarser microstructures (Sadiq *et al.*, 2013). To overcome these problems, and to further improve the reliability of solder joints, different elements and/or micro or nanoparticles have been added to change the microstructure and enhance other properties (Sona and Prabhu, 2013). In this review, the impact of adding different elements/nanoparticles and other materials on the *MP*, microstructure, mechanical properties and wettability of all *SAC* family members is presented.

2. Melting point

Melting temperature *(MT)* is one of the most important properties for the development of *LFSs* (El-Daly and Hammad, 2012). *MT* is the liquidus temperature (T_L) making the solder alloy completely molten, which is necessary for soldering operations (Abtew and Selvaduray, 2000). The *MT* is essential to develop better solder joints and occurs if the solidus temperature (T_S) is low (Mei *et al.*, 1996) because rapid solidification can provide a better and more refined microstructure which has a direct impact on a solder joint's strength (Kanlayasiri *et al.*, 2009). Moreover, a good solder alloy should have a narrow melting range $(\Delta T = T_L - T_S)$ and low *MT* (El-Daly and Hammad, 2012). Taking into account that a conventional eutectic *Sn-Pb* solder melts at 183°C, this can be considered as the benchmark for new *LFSs* (Jeon *et al.*, 2008). However, the *MP* of *SAC* is approximately 217°C, which results in thicker *IMCs* than those of *Sn-Pb*. Therefore, some researchers have added alloying elements, or nanoparticles, to reduce the *MT* of the *SAC* series. For instance, Kanlayasiri *et al.* (2009) reported that the doping of indium (*In*) into *SAC* lowers the T_S and T_L. Their results concluded that, upon addition of 3 Wt.% *In* to *SAC*, T_S (219.4°C) and T_L (241.7°C) decreased by 21.7°C and 11.5°C, respectively. Subsequently, the difference between T_S and T_L of the *SAC* increased from 22.3 °C to 32.5 °C. However, *In* is expensive and it increases the cost of *LFSs*. Chuang *et al.* (2012) investigated the influence of titanium *(Ti)* on the *MT* of *SAC*. Their results showed that the addition of 1.0 Wt.% of *Ti* into *SAC* decreased the T_S and T_L from 216.92°C and 221.58°C to 216.59°C and 219.47°C, respectively. In addition, the melting range of *SAC* also decreased from 4.66°C to 2.88°C. A narrow melting range is one of the desirable thermal properties of solders, meaning they exist in the liquid form only for a very short time during solidification for the formation of acceptable joints. In another study by Shnawah *et al.* (2013), differential scale calorimetry (*DSC)* analysis was used to check the thermal behaviour of *SAC* after the addition of iron (*Fe)*. They found that 0.6 Wt.% of *Fe* gave a lower *MP* by showing one endothermic peak at 221.35°C at a eutectic composition. Huang and Wang (2005) also reported a decrease in the *MP* of *SAC* upon addition of bismuth (*Bi)*. According to their findings, the T_S of *SAC-2Bi* and *SAC-4Bi* were 213.08°C and 206.40°C, respectively. However, peeling of the solder joint appeared when the *Bi* addition was > 4 Wt.%.

Furthermore, the addition of Rare-Earth (*RE)* elements (Wu and Wong, 2007) and nanoparticles (Efzan Mhd Noor *et al.*, 2013) have also contributed better properties to SAC, while not drastically affecting the *MP*. For instance, Dudek and Chawla (2010) studied the *DSC* curves of *SAC* and *SAC*-0.5*RE*. Their selected *RE* elements were lanthanum *(La)*, cerium *(Ce)*, and yttrium *(Y)*, where it was found that all solders *(La, Ce, and Y)* displayed a single endothermic peak between 217°C and 219°C. Liu *et al.* (2008) studied the minor addition of silicon carbide (*SiC)* nanoparticles to the *SAC* and found that it did not change its *MT* noticeably. However, upon the addition of only 0.2 Wt.% *SiC*, a lower *MP* value was observed as the endothermic peak shifted from 219.9°C to 218.9°C. Tsao *et al.* (2013) analysed *DSC* curves of *SAC* doped with aluminium oxide (Al_2O_3) nanoparticles. It was found that the *MP* of *SAC*, which was 221.2°C, slightly increased as the amount of Al_2O_3 nanoparticles increased. Gain *et al.* (2011) also observed no significant change in the *MP* of *SAC* with 1 Wt.% *of titanium dioxide* (TiO_2) nanoparticles. It was concluded that *DSC* analyses gave only a eutectic peak from 217.00°C to 217.64°C. Similar behaviour was noted in another study by Chang *et al.* (2011). In conclusion, adding alloying elements and nanoparticles to *SAC* alloys had little effect on the *MT*.

3. Microstructure

A thin layer of *IMCs* is required to attain a better metallurgical bond for the reliability of electronic solders; however, their higher growth has undesirable impacts on the mechanical properties due to their brittle nature (Liang *et al.*, 2014). Therefore, it is important to expand the knowledge of *IMCs* for the reliability of solder interconnections (Aamir *et al.*, 2017c; Aamir *et al.*, 2019). In this review, the addition of alloying elements etc into *SAC* alloys is discussed to highlight the impact of precipitates in suppressing the growth of *IMCs* for refined and uniform microstructures.

Chuang *et al.* (2012) concluded that, after the addition of different amounts of *Ti* into *SAC*, the microstructure became uniform due to the active properties of *Ti*, which gave rise to heterogeneous *IMCs* and reduced the dendritic size. However, it was recommended that the *Ti* concentration should not exceed 1.0 Wt.%, which in turn gave rise to coarse Ti_2Sn_3 in the eutectic colonies and made the microstructure worse. Sabri *et al.* (2013) found that inclusions of aluminium (*Al)* in

SAC led to the arrangement of a large amount of additional *Ag_3Al* and *Al_2Cu IMCs*. These *IMCs* possessed snowflake, circle, rod, and quadrangle shaped morphologies and were lightly distributed within the microstructures located in and at the vicinity of interdendritic regions. Moreover, these additional *IMCs* refined the microstructure of *SAC* by restraining the growth formation of *IMCs* (*Ag_3Sn* and *Cu_6Sn_5*). In another study by Leong and Haseeb (2016), the effect of a minor addition of *Al* into *SAC* on the interfacial structure between the solder and copper substrate during reflow was investigated. It was determined that the minor addition of *Al* into *SAC* formed small equiaxed *Cu-Al* particles, *Cu_3Al_2*, which suppressed the growth of the interfacial *Cu_6Sn_5 IMC* after reflow. Zhang *et al.* (2012a) investigated doping of zinc *(Zn)* into *SAC*, which remarkably refined the microstructure with the condition that concentrations of *Zn* should be limited to 0.8 Wt.%. The refinement in microstructure was due to the formation of dispersed *Cu-Zn IMCs* which reduced the thickness of the *IMCs* and ultimately changed the morphology. Hammad (2013) found that adding 0.05 Wt.% *Ni* into *SAC* formed *$(Cu, Ni)_6Sn_5$ IMCs* in the eutectic regions, which decreased the inter-particle spacing and resulted in a more refined morphology. Wang *et al.* (2019) fabricated *SAC* with 0.2 Wt.% zirconium *(Zr)* using a vacuum induction melting method. Their study demonstrated that *Zr* refined the microstructure of *SAC* by reducing the size of the *IMCs*, which further participated in improving the strength of the solder alloy. Moreover, 0.2 *Zr* Wt.% gave significantly better results, even after isothermal aging. However, no change in the melting range was observed.

RE elements are good surface-active agents and are considered vital materials for improving the microstructure and mechanical properties (Sadiq *et al.*, 2013). They can accumulate at grain/dendrite boundaries and can lower the energy of the grain/dendrite boundary by restricting the motion of the boundaries. Thus, they restrict the growth of *IMCs* and give a refined microstructure (Xia *et al.*, 2002). Dudek and Chawla (2010) reported that *RE* addition into *SAC* produced *RE*-containing particles, i.e. *$RESn_3$ IMC*, apart from *Cu_6Sn_5* and *Ag_3Sn*, which were responsible for the refinement of the microstructure as shown in Figure 1.

In addition, Yasmin and Sadiq (2014) concluded that the appropriate composition of *La* in *SAC* reduced the grain size and provided better microstructure by effectively suppressing the growth rate of *IMCs* (*Ag_3Sn* and *Cu_6Sn_5*) even during thermal ageing. This refinement in the *SAC* microstructure was due to the aggregation of *La* at the interface, which provided blockage for the production of large *IMCs*. The same recommendation was made in another study by Sadiq *et al.* (2013). Moreover, a careful examination of the microstructure after *Ce* inclusion in *SAC* was done by W Chen *et al.* (2011). Their results showed that adding *Ce* promoted the formation of *Ce-Sn IMCs* which acted as a blockage to decrease the growth of *Ag_3Sn* and *Cu_6Sn*; thus, giving a refined microstructure. Zhang *et al.* (2012b) also studied the contribution of 0.03 Wt.% *Ce* in *SAC*. Their study showed that the activation energy for the growth of *IMCs* was higher for *Ce*-based *SAC*, which was responsible for reducing the growth of *IMCs* and increasing the strength of the solder joint. Furthermore, Tu *et al.* (2017) reported that 0.15 Wt.% of *Ce* in *SAC* improved the microstructure by reducing the thickness of the *IMC*s. Zhang *et al.* (2014) reported that additions of 0.05 Wt.% of ytterbium (*Yb*) in *SAC* improved the properties for electronic packaging and refined the microstructure by retarding the growth of *IMCs* during soldering. In another study (Gao *et al.*, 2010b), the incorporation of a small concentration of praseodymium (*Pr*) in *SAC* was shown to produce extra *$PrSn_3$* particles which restricted the *IMC* growth because of the heterogeneous nucleation by lowering the reaction time of the liquid solder with the substrate. However, more than 0.05 Wt.% of *Pr* resulted in the arrangement of the bulk *$PrSn_3$* compound.

Figure 1 *SEM* micrographs of (a) *SAC* with the addition of 0.5 Wt.% of (b) *La*, (c) *Ce* and (d) *Y*

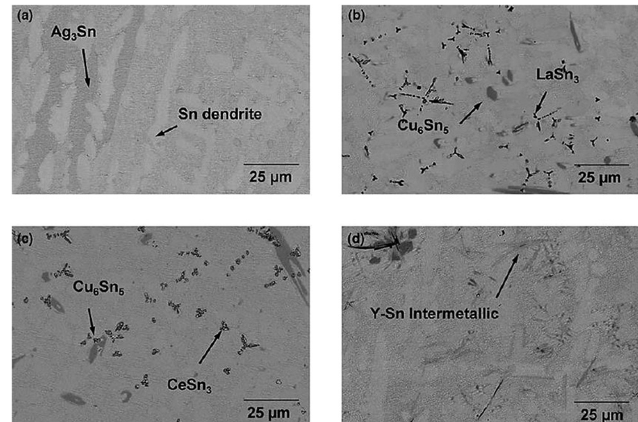

Source: Dudek and Chawla (2010)

Nanoparticles also play a vital role in changing the microstructure of *SAC* alloys. For instance, Liu *et al.* (2008) concluded that the inclusion of 0.05 Wt.% *SiC* nanoparticles remarkably decreased the average grain size, due to the strong adsorption effect and high surface free energy, which led to refined *IMCs*. Sharma *et al.* (2019) used a simple mechanical blending and casting method to add zirconia (*ZrO_2*) nanoparticles to *SAC*. It was concluded that, after the addition of *ZrO_2* nanoparticles, the thickness of the grain size, and *IMCs* such as *Ag_3*Sn and *Cu_6Sn_5* were refined by 46 per cent, 14 per cent, and 26 per cent, respectively compared to the original *SAC* alloy. Bashir *et al.* (2016) used a nanoparticle-doped flux technique to add 2 Wt.% *Co* nanoparticles into *SAC*. The influence of the *Co* nanoparticle-doped flux was then investigated with an electro-migration *(EM)* test performed in an oil bath at 80°C for a duration of 1128 h with a current density of 1×10^4 A/cm^2. Their study concluded that the presence of 2 Wt.% *Co* nanoparticles in *SAC* restricted the size of the *IMCs*, both at the cathode and anode sides. In addition, the tensile strength of the solder joint increased after the addition of *Co* nanoparticles when the *EM* test was performed at 150°C for 0 h and 192 h. This study showed that a 2 Wt.% *Co* nanoparticle-doped flux improved the reliability of *SAC* solder joints. Sujan *et al.* (2017) also worked on the addition of *Co* nanoparticles using the flux doping technique. This method is useful with surface mount technology and does not require any further steps in the manufacturing line. Their results showed that the addition of *Co*-nanoparticles with an average

size of 58 nm into *SAC* stabilised the formation of Cu_6Sn_5 *IMC* and improved the growth of *Co* containing *IMCs*. Haseeb *et al.* (2017) provided an overview to discuss the effects of metallic nanoparticles on the characteristics of interfacial *IMCs* in *Sn*-based solder joints on *Cu* substrates during reflow and thermal aging. The *Ni, Co, Zn, Mo, Mn*, and *Ti* nanoparticles were mechanically blended with the *SAC* solder paste. It was shown that, through the paste mixing route, the *Ni, Co, Zn* and *Mn* nanoparticles greatly contributed to changing the morphology and reducing the thickness of the *IMCs*, which helped the solder joint to perform in a favourable way. Basak *et al.* (2018) investigated the addition of minor amounts of *Fe or* Al_2O_3 nanoparticles into *SAC*. Their results indicated that supplements of *Fe* nanoparticles formed $FeSn_2$, together with the *IMCs* of *SAC* alloy, i.e. Ag_3Sn and Cu_6Sn_5, which stopped the growth of grains/*IMCs* during aging/reflowing. However, Al_2O_3 nanoparticles did not participate in phase formation but acted as a grain refiner. Yakymovych *et al.* (2017) added *Ni* nanoparticles into *SAC* using a cold-pressing method in which powders of *SAC* and *Ni* nanopowders were mixed mechanically, and processed into 8 mm diameter rods. It was observed that the presence of *Ni* nanoparticles in *SAC* formed a $(Cu, Ni)_6 Sn_5$ phase which participated in the refinement of the microstructure due to the fine distribution of *IMCs* in the *Sn* matrix. Gain and Zhang (2019) found that 0.5 Wt.% *Ni*-nanoparticles in *SAC* produced new *(Cu, Ni)-Sn IMC* phases as shown in Figure 2. The new *IMC* phase refined the microstructure of *SAC* and improved the mechanical reliability of electronic interconnections which, subsequently, enhanced the lifespan of miniaturised electronic products.

Carbon nanotubes *(CNTs)* have been acknowledged as offering better physical, electrical and mechanical properties, which make them suitable for the fabrication of novel composites (Nai *et al.*, 2008). Zhu *et al.* (2018) worked on doping *CNTs* with three different ranges of diameters, 10-20, 40-60, and 60-100 nm, into *SAC* (Figure 3). Their studies concluded that the addition of *CNTs* into *SAC* provided better performance. Among all, the addition of *CNTs* in *SAC* in the range of diameter (40-60 nm) produced a refined microstructure by lowering the growth rate of the *IMCs* up to 30.9 per cent. The refinement in microstructure was attributed to the agglomeration and adsorption of *CNTs* in the solder matrix and *IMCs* interface.

Kumar *et al.* (2008) concluded that adding single-walled carbon nanotubes (*SWCNT)* into *SAC* played a significant role in reducing the average size of the *IMCs* due to the dispersion of nanotubes at the grain boundaries of the Ag_3Sn, which resulted in a uniform morphology. Xu *et al.* (2015) studied the impact of graphene-nano-sheets (*GNSs)* on *SAC*. Their study found that *GNSs* participated in restricting grain growth and gave fine *IMCs*. The average sizes of the *IMCs*, after addition of 0.03, 0.07, and 0.10 Wt.% *GNSs* reduced to 1.35, 1.24 and 1.21 μm, respectively, compared to1.96 μm for *SAC*. All these reduced size *IMCs* played a vital role in enhancing the solder joint reliability.

Overall, the addition of an appropriate composition of alloying elements, nanoparticles and composites can significantly change the microstructure of *SAC* alloys. However, the addition of more than a critical composition can negatively impact the properties of the solder joints. Therefore, selecting the optimum doping concentrations is highly recommended.

4. Mechanical properties

Alloying elements and nanoparticles also play a significant role in improving the mechanical properties of *SAC* alloys (Sun and Zhang, 2015). Table I shows the impact of adding alloying elements, nanoparticles or other materials on the mechanical properties of *SAC*.

Chuang *et al.* (2012) found that up to 1.0 Wt.% of *Ti* in *SAC* improved the mechanical properties. Their study also concluded that excess concentrations of *Ti* produced coarse Ti_2Sn_3 in the eutectic colonies which, subsequently, degraded the mechanical properties of *SAC*. Fallahi *et al.* (2012) determined that adding 0.2 Wt.% and 0.6 Wt.% of *Fe* increased the shear strength of *SAC* up to 40 MPa and 53 MPa, respectively. Zhang *et al.* (2012a) concluded that the addition of 0.8 Wt.% of *Zn* increased the strength of the *SAC*. However, more than 0.8 Wt.% of *Zn* gave disperse *Cu-Zn IMCs*, which resulted in coarsening of the microstructure because of the

Figure 2 *SEM* images of (a) *SAC* and (b) SAC-0.5 Wt.% nanosized *Ni* particles

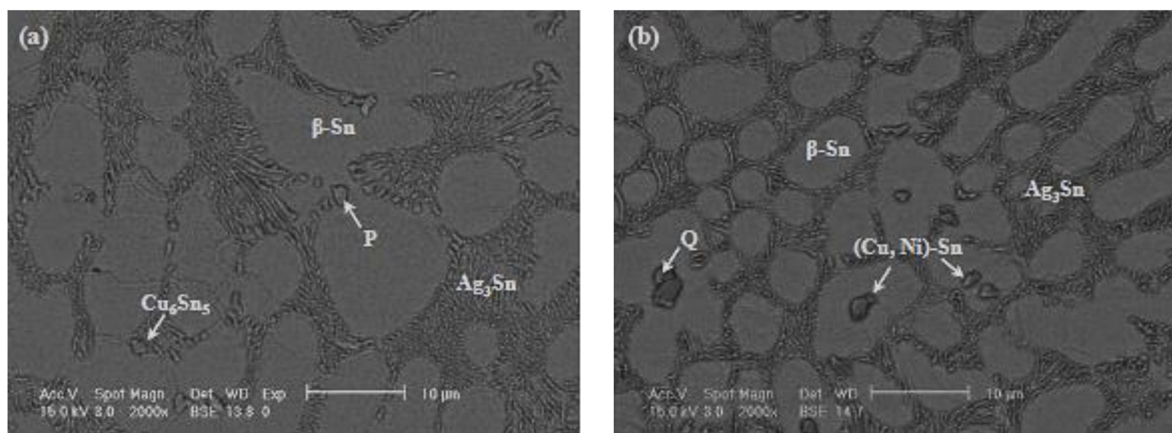

Source: Gain and Zhang (2019)

Figure 3 (a) Schematic diagram of *MWCNTs* structure and *TEM* images of *CNTs*: (b) 10-20 nm, (c) 40-60 nm and (d) 60-100 nm

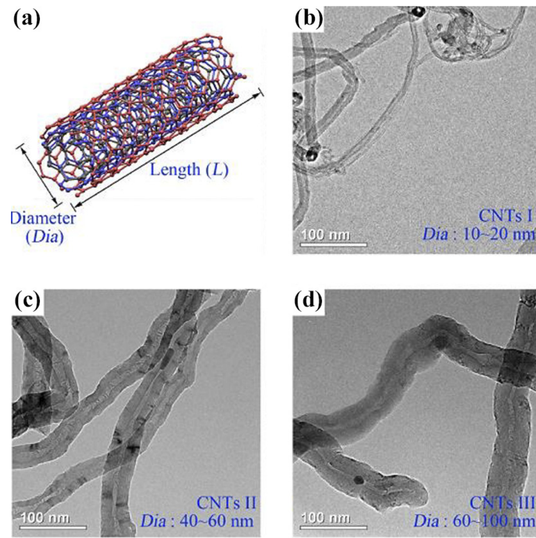

Source: Zhu *et al.* (2018)

great affinity of *Zn* towards oxygen. Therefore, an excessive *Zn* content resulted in the formation of ZnO_2 which untimely reduced the tensile strength. El-Daly and El-Taher (2013) reported that *YS*, *UTS*, and the ductility of *SAC* were improved after the addition of 0.05 Wt.% of *Ni* because of the refined microstructure. However, addition of 0.1 Wt.% of *Ni* into *SAC* resulted in an abrasive microstructure which in turn degraded the mechanical properties. Li *et al.* (2006) and Chen and Li (2004) found, in their studies, that doping of *Sb* also improved the tensile strength of *SAC*. This improvement in strength was due to the reduced size of *IMCs* which ultimately refined the microstructure. The same investigation was detailed by Hammad (2018), who recommended adding 0.5 Wt.% of *Sb* into *SAC* to improve the mechanical strength and ductility of the solder joint. In another study by Luo *et al.* (2014), the addition of up to 0.5 Wt.% of *Ga* was recommended to improve the shear strength of *SAC* by 17.9 per cent.

Regarding *RE* elements, Ali (2015) concluded that the optimum *La* concentration in *SAC* for desired mechanical properties including *YS*, *UTS* and ductility was 0.3 Wt.%. Aamir *et al.* (2017b) reported that better mechanical properties could be obtained when the *La* composition was less than 0.4 Wt.%, even after thermal ageing. Hao *et al.* (2007) found improvement in the strength of *SAC* after the addition of *Y*; however, the joint strength decreased dramatically for *Y* concentrations beyond 0.15 Wt.%. Shi *et al.* (2008) reported that adding $\leq$0.1 Wt.% *Er* to *SAC* increased the shear strength significantly, due to the reduced size of Ag_3Sn and Cu_6Sn_5. Gao *et al.* (2010a) concluded that, when the *Nd* supplement was 0.05 Wt.%, the pull force and sheer force of the solder joint was improved by 19.4 per cent and 23.6 per cent, respectively. The improvement in pull force and sheer force was due to the refinement in the *IMCs* by *Nd*. Their study also suggested that the amount of *Nd* in *SAC* should not exceed 0.25 Wt.%. In another study by Gao *et al.* (2010b), the addition of up to 0.05 Wt.% of *Pr* also increased both the pull force and sheer force by 18.5 per cent and 19.4 per cent, respectively. Similarly, Zhang *et al.* (2014) reported that inclusions of 0.05 Wt.% *Yb* to the *SAC* increased the tensile force of *SAC* solder joints by 25.4 per cent. Tu *et al.* (2017) concluded that addition of 0.15 Wt.% of *Ce* into *SAC* improved *E*, *YS* and *UTS* of *SAC*. Furthermore, *SAC-0.15Ce* also gave better shear strength, even after thermal ageing, as shown in Figure 4.

Tsao *et al.* (2013) concluded that the addition of 1.0 Wt.% of Al_2O_3 nanoparticles increased the shear strength of *SAC* after 1 and 8 reflow cycles by 14.4 per cent and 16.5 per cent, respectively. Tang *et al.* (2014) added different compositions of TiO_2 nanoparticles into *SAC* which improved the mechanical properties at the 0.1 Wt.% level. The improvement was due to refinement of the microstructure after the reduced space between the Ag_3Sn *IMCs*. Bashir *et al.* (2016) concluded that a 2.0 Wt.% Co nanoparticle-doped flux improved the reliability of *SAC* solder joints because their tensile strengths increased after 0 h as well as 192 h of *EM* testing at 150°C. Gain and Zhang (2018) reported that adding 1.0 Wt.% of TiO_2 nanoparticles into *SAC*, prepared by a mechanical mixing process, enhanced the creep and shear strength. It was also noted that the Cu_6Sn_5 and Cu_3Sn phases were observed on the *Cu* substrate through interfacial structure characterisation, and a ternary *(Cu, Ni)-Sn* phase had grown on an *Au*/N*i*-plated *Cu* pad of a Ball Grid Array. These *IMCs* started growing during thermal aging, however, TiO_2 nanoparticles suppressed the growth of the *IMC*s and thus, the creep, shear strength and thermal shock resistance were improved. Gain and Zhang (2019) found that, in addition to the improvement in electrical properties, the elastic modulus, shear modulus, and microhardness were also improved by 8 per cent, 11.2 per cent, and 16.7 per cent, respectively, when the addition of *Ni*-nanoparticles into *SAC* was 0.5 Wt.%. The reason for the overall good properties of the solder joints was the appearance of relatively fine *IMCs* dispersed in a β*-Sn* matrix and the fine microstructure. Roshanghias *et al.* (2012) recommended that the best combination of mechanical properties was achieved with 0.75 Wt.% of CeO_2 nanoparticles int *SAC*. Nai *et al.* (2006) suggested that the addition of 3.0 Vol.% of titanium diboride (TiB_2) nanoparticles resulted in improved levels of *YS* and *UTS* by 26 per cent and 23 per cent, respectively. Yang *et al.* (2014) concluded that adding 0.05 Wt.% *Ni*-coated carbon nanotubes (*Ni-CNTs)* into *SAC* significantly improved the tensile strength. The prime reason for its better tensile strength was that the *CNTs* obstructed the start of dislocation motion in the *SAC*. Kumar *et al.* (2008) concluded that 1.0 Wt.% of *SWCNT* enhanced the *UTS* of *SAC* up to 50 per cent. Zhu *et al.* (2018) also found that the reinforcement of *CNTs* in *SAC* improved *E*, *YS*, and *UTS*. The recommended range of the diameter of the *CNTs* was 40-60 nm, which contributed to reducing the growth of *IMCs* and thus, provided superior mechanical properties. Furthermore, upon addition of 0.03 Wt.% of *GNSs*, the *UTS* of *SAC* was improved by ~10 per cent, because of the refined microstructure due to the reduced average size of the *IMCs* (XD Liu *et al.*, 2013). Overall, the use of alloying elements and nanoparticles significantly contributed to the refinement of microstructure and improved mechanical properties of *SAC* series solders. However, it should be noted that

Table I Role of the fourth element in the mechanical properties of *SAC*

Alloying element	Composition weight percentage	Mechanical properties	References
Ti	Up to 1.0 Wt.%	Increase the *YS, UTS*, and microhardness of *SAC*	Chuang *et al.* (2012)
Fe	0.6 Wt.%	Shear strength of *SAC* increases up to 53 MPa from 29 MPa	Fallahi *et al.* (2012)
Zn	0.8 Wt.%	Improves the tensile force of *SAC* joints by 10%	Zhang *et al.* (2012a)
Ni	0.5 Wt.%	Improves *YS, UTS* and ductility of *SAC*	El-Daly and El-Taher (2013)
Sb	0.5 Wt.%	Gives higher strength and ductility	Hammad (2018)
Ga	Up to 0.5 Wt.%	Improves the shear strength of *SAC* solder joints up to 17.9%	Luo *et al.* (2014)
La	0.3 Wt.%	Increases in *YS, UTS* and ductility are found which then improve toughness, creep and fatigue resistance of the *SAC*	Ali (2015)
Y	$<$0.15 Wt.%	The strength of the *SAC* joint is improved	Hao *et al.* (2007)
Er	$\leq$0.1 Wt.%	Shear strength of *SAC* solder is improved by 18 %	Shi *et al.* (2008)
Nd	0.05 Wt.%	Pull force and sheer force of *SAC* joint are increased by 19.4 % and 23.6 %, respectively	Gao *et al.* (2010a)
Pr	0.05 Wt.%	Improves pull force and sheer force of *SAC* solder	Gao *et al.* (2010b)
Yb	Up to 0.05 Wt.%	The tensile force of the *SAC* solder joint increase by 25.4%	Zhang *et al.* (2014)
Ce	0.15 Wt.%	Increase the shear strength, ductility, *E, YS*, and *UTS*	Tu *et al.* (2017)
Al Nanoparticles	3.0 Wt.%	Improves the shear strength of *SAC*	Gain *et al.* (2010)
Al_2O_3 Nanoparticles	1.0 Wt.%	The shear strength after 1 cycle and 8 cycles of reflow is increased by 14.4 % and 16.5 %, respectively	Tsao *et al.* (2013)
TiO_2 Nanoparticles	0.1 Wt.%	Gives better microhardness and tensile properties	Tang *et al.* (2014)
CeO_2 Nanoparticles	0.75 Wt.%	Improves *YS* and *UTS* of *SAC*	Roshanghias *et al.* (2012)
TiB_2 Nanoparticles	3 Vol.%	Increase *YS* and *UTS* by 26 % and 23 %, respectively	Nai *et al.* (2006)
***Co-* nanoparticles**	2 Wt.%	Increases the tensile strength of *SAC*	Bashir *et al.* (2016)
***Ni*-nanoparticles**	0.5 Wt.%	The elastic modulus, shear modulus and microhardness increase by 8.0 %, 11.2 % and 16.7 % in *SAC*, respectively.	Gain and Zhang (2019)
Ni-CNTs	0.05 Wt.%	Improves the tensile strength of *SAC* solder slabs and joints	Yang *et al.* (2014)
SWCNT	1.0 Wt.%	Increases the *UTS* of *SAC* up to 50 %	Kumar *et al.* (2008)
MWCNT	10-60 nm	Improvements in *E, YS* and *UTS* of *SAC* were found	Zhu *et al.* (2018)
GNSs	0.03 Wt.%	Increased the *UTS* of *SAC* solder by approximately 10 %	Liu *et al.* (2013)

there was also an appropriate maximum concentration beyond which those properties degraded.

5. Wettability

Wettability testing is used to examine the wetting properties that include surface tension and wetting force (Sadiq, 2012). Traditional *Sn-Pb* solder has better wettability due to the presence of *Pb* (Dharma *et al.*, 2009; Wu *et al.*, 2004). Thus, when changing from *Sn-Pb* to *LFS*, wettability becomes an important concern. Furthermore, most of the *LFS* alloys have good mechanical properties when tested in bulk but their wetting, when soldered on boards, is not good for the reliability of solder joints. This means that wettability, or solderability, is necessary for characterising the solder alloys and becomes important when high solder joint reliability is required (Sadiq, 2012).

There are two well-known tests used to characterise the wettability of solder: the spread area test and the wetting balance test (Wu *et al.*, 2004). In the spread area test, a solder disc is coated with flux, melted, and allowed to solidify on a substrate. When a bond is formed, the free energy is reduced and hence the solder changes its shape (Wu *et al.*, 2004). This change in shape causes an increase in the contact area which shows the wetting behaviour of the solder. In some cases, the ratio of the as-bonded area to this new area (after soldering) is taken as the wettability of the solder (Wu *et al.*, 2004). Wetting balance testing is another important technique for evaluating solder wettability. In this method, a coupon (for example *Cu*) is dipped into the molten solder. The molten solder moves up the coupon because of the wetting force exerted on it. Different forces, due to buoyancy, come into action after partial dipping of the coupon into the solder bath, including the surface tension, which are quite high at the solder/flux interface. The resultant force is then the measurement of the meniscus and the wetting angle (Sadiq, 2012).

In investigations into improving the wettability of *SAC*, the addition of *RE* elements was the most noticeable (Xiong and Zhang, 2019). The wetting properties of *SAC* and *SAC-La* at 250°C were investigated by Sadiq (2012). It was noticed that the surface tension of *SAC* decreased due to *La* doping. The wetting force of *SAC* was 5.7 mN, which increased up to 6.7 mN for *SAC*-0.25*La* as shown in Figure 5(a). However, when the *La* content increased to 0.5 Wt.%, the wetting force showed a lower value than *SAC*-0.25*La*. Thus, the addition of *La* in *SAC* beyond 0.25 Wt.% decreased the wetting force, ultimately affecting the wettability. Therefore, the optimum level of *La* in *SAC* should be considered as 0.25 Wt.%. In the same study, wetting or contact angle were found on the basis of the surface tensions. An appreciable decrease in contact angle was noted with *SAC*-0.25*La* having a better (smaller) contact

Figure 4 Mechanical properties of *SAC* with different levels of *Ce*

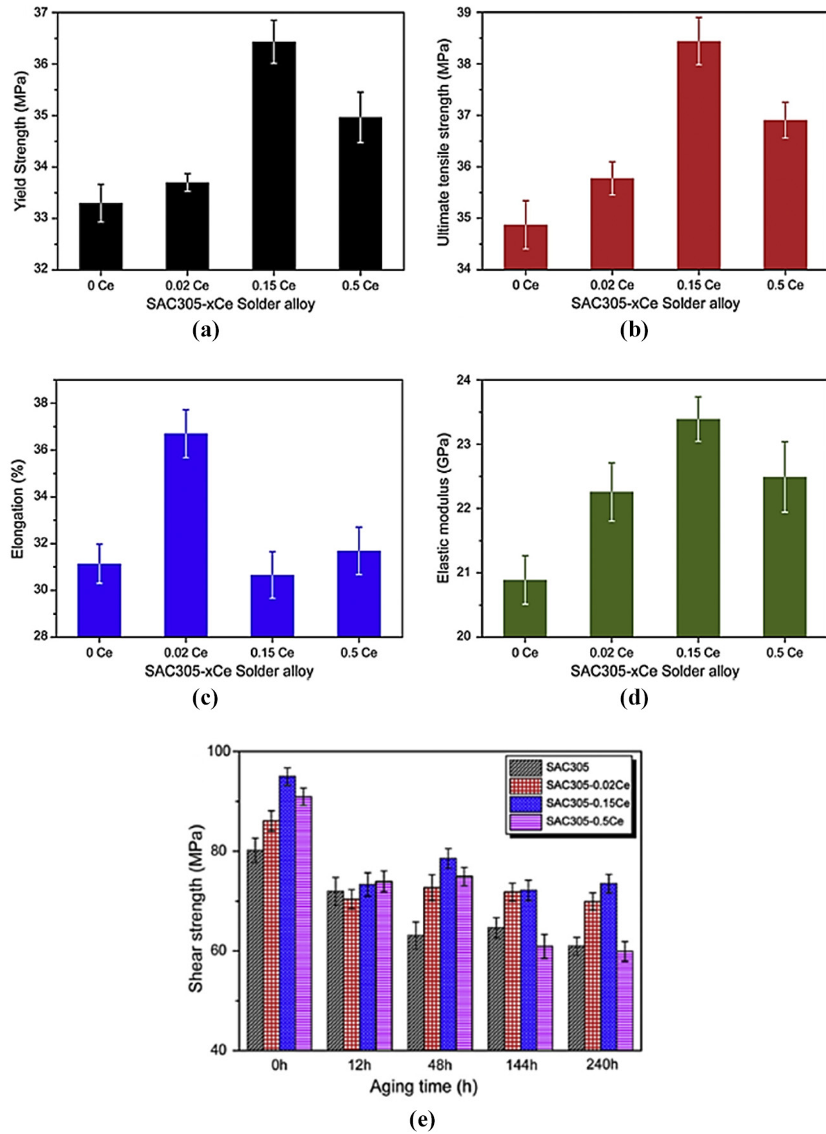

Source: Tu *et al*. (2017)

Figure 5 *SAC* and *SAC-La* at 250°C

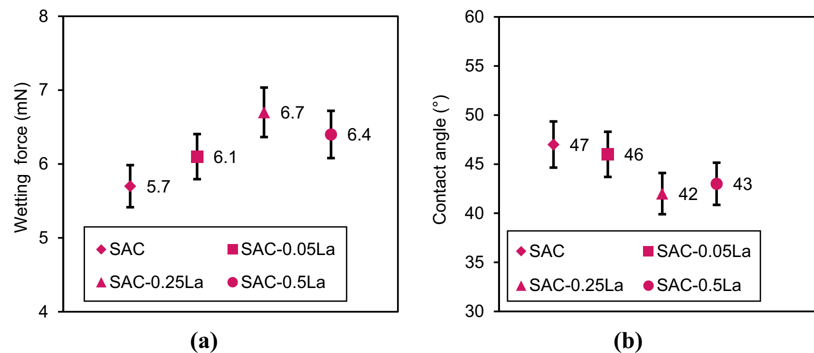

Notes: (a) Wetting forces; (b) contact angles Sadiq (2012)

angle than *SAC* and *SAC*-0.5*La* alloys. Figure 5(b) shows that *SAC*-0.25*La* decreased the wetting angle of *SAC* from 47° to 42° and again *SAC-0.5La* showed a larger wetting angle than *SAC*-0.25*La*. Therefore, the optimum doping of *La* in *SAC* was 0.25 Wt.%, as beyond this the wetting angle increased, ultimately affecting the wettability.

Gao *et al.* (2010a) concluded that trace amounts of *Nd* remarkably improved the wetting behaviour of *SAC*. Figures 6(a) and (b) show the wetting time and wetting force of *SAC-Nd* at different temperatures, which clearly show that the wettability of *SAC* improved with 0.05 Wt.% of *Nd* because of its lower surface tension. Gao *et al.* (2010b) in another study also reported that 0.05 Wt.% of *Pr* improved the wetting properties of *SAC*. Figure 7 shows that the highest spreading area was 63.27 mm, which was observed for *SAC-0.05Pr*.

Furthermore, the wettability of *SAC-Ce* was studied by Wang *et al.* (2009). They concluded that, after the addition of *Ce*, the wetting behaviour of *SAC* improved significantly. The observed wetting time was ~0.7 *s* at 250°C, which was very close to that of *Sn-Pb* solder.

Nanoparticles can also improve the performance of *SAC*. Tay *et al.* (2013) concluded that adding *Ni* nanoparticles into *SAC* increased the wetting angle from 19.3° to 29.9°. Yoon *et al.* (2005) reported that *Co* nanoparticles in *SAC* increased the wetting angle, but decreased the spreading rate. Similar effects with *Co* nanoparticles were reported by Haseeb and Leng (2011). Tsao *et al.* (2010) found that 0.5 Wt.% of Al_2O_3 nanoparticles had the same effect on the wetting behaviour of *SAC*, giving a minimum contact angle of 28.9°. Li *et al.* (2014) produced mechanically mixed TiO_2 nanoparticles in *SAC*. Their study showed that adding 0.25 Wt.% of TiO_2 nanoparticles decreased the wetting time by 53.7 per cent, while the wetting force increased to 37.6 per cent. Kanlayasiri and Meesathien (2018) reported that the maximum wettability of *SAC* was achieved with 0.25 Wt.% of zinc oxide (*ZnO*) nanoparticles. Jung *et al.* (2018) worked on different compositions of TiO_2 and Graphene. All compositions were mixed simultaneously at equal weight fractions into *SAC* molten solder by a mechanical mixing method and melting, to produce a bulk nanocomposite solder. Their results showed that a 0.21 Wt.% nanomaterial addition gave with had wettability and spreadability improvements of 33.67 per cent and 8.66 per cent, respectively.

Figure 7 Effect of *Pr* on the solderability of *SAC*

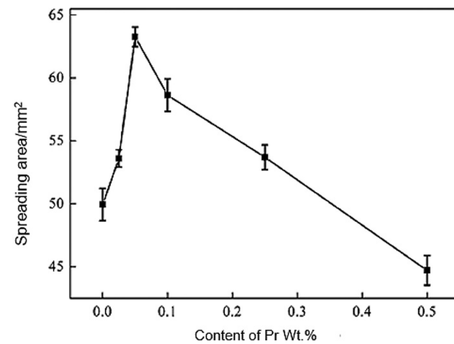

Source: Gao *et al.* (2010b)

6. Conclusions

Lead-free solder alloys are considered to be one of the most important segments of the global green electronics environment. The most commonly used lead-free solder alloys are *SAC* as they offer good mechanical properties comparison to conventional tin-lead. Addition of alloying elements or a composite approach can overcome limitations of these *SAC* solders, especially the microstructure, mechanical properties, and wettability. However, no significant effect on the MP was observed and thus, no adjustment should be required in the reflow process to meet the requirement of the present soldering process. Further research is required to ensure that the addition of alloying elements or a composite approach can decrease the MP of tin-silver-copper. Moreover, it is worth noting that the addition of a fourth element or nanoparticles is actively involved in refining the microstructure, giving good mechanical properties and wettability, (with the condition that the added compositions should not be in an excess amount for the solder joint's reliability). In this regard, when developing new lead-free solder alloys, the optimum concentration of the material added to the tin-silver-copper should be carefully examined. Future studies should aim to determine the optimal additive

Figure 6 Effect of *Nd* on the solderability of *SAC* solders

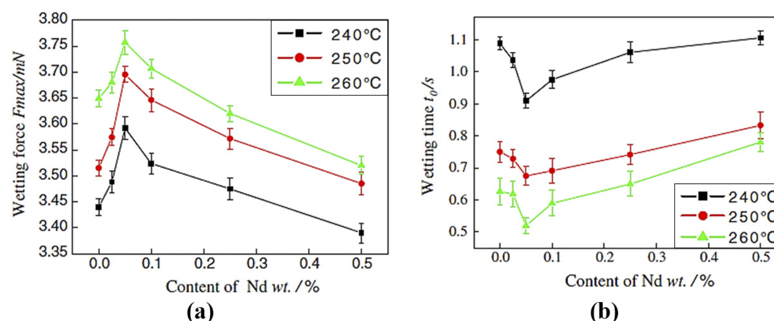

Notes: (a) Wetting force; (b) wetting time
Source: Gao *et al.* (2010a)

compositions that can improve the thermal behaviour, interfacial reactions, tin whiskering, wettability, microstructure and mechanical properties of SAC alloys. Moreover, the work should also be extended to find the desired inclusions into tin-silver-copper that can effectively exhibit better performance under different strain rates and, thermal ageing at different times and temperatures.

References

Aamir, M., Muhammad, R., Ahmed, N. and Alam, K. (2015), "Impact of thermal aging on microstructure and mechanical properties of high Sn content, Sn-Pb solders", *Fourth International Conference on Aerospace Science & Engineering, Islamabad, Pakistan, Institute of Space Technology, 2015, Islamabad, Pakistan*, Institute of Space Technology, *Islamabad*, pp. 187-191.

Aamir, M., Muhammad, R., Ahmed, N. and Waqas, M. (2017b), "Impact of thermal aging on the intermetallic compound particle size and mechanical properties of lead free solder for green electronics", *Microelectronics Reliability*, Vol. 78, pp. 311-318.

Aamir, M., Muhammad, R., Ahmed, N., Sadiq, M. and Waqas, M. (2017a), "Mechanical properties of lead free solder alloy for green electronics under high strain rate and thermal aging", *Journal of Engineering and Applied Sciences (JEAS)*, Vol. 36 No. 1, pp. 115-123.

Aamir, M., Waqas, M., Iqbal, M., Hanif, M.I. and Muhammad, R. (2017c), "Fuzzy logic approach for investigation of microstructure and mechanical properties of Sn96.5-Ag3.0-Cu0.5 lead free solder alloy", *Soldering & Surface Mount Technology*, Vol. 29, pp. 191-198.

Aamir, M., Tolouei-Rad, M., Din, I.U., Giasin, K. and Vafadar, A. (2019), "Performance of SAC305 and SAC305-0.4La lead free electronic solders at high temperature", *Soldering & Surface Mount Technology*, Vol. 31, pp. 250-260.

Abtew, M. and Selvaduray, G. (2000), "Lead-free solders in microelectronics", *Materials Science and Engineering: R: Reports*, Vol. 27 Nos 5/6, pp. 95-141.

Ali, B. (2015), "Advancement in microstructure and mechanical properties of lanthanum-doped tin-silver-copperlead free solders by optimizing the lanthanum doping concentration", *Soldering & Surface Mount Technology*, Vol. 27, pp. 69-75.

Basak, A., Pramanik, A., Riazi, H., Silakhori, M. and Netting, A. (2018), "Development of Pb-free nanocomposite solder alloys", *Journal of Composites Science*, Vol. 2 No. 2, pp. 28.

Bashir, M.N., Haseeb, A., Rahman, A.Z.M.S. and Fazal, M. (2016), "Effect of cobalt doping on the microstructure and tensile properties of lead free solder joint subjected to electromigration", *Journal of Materials Science & Technology*, Vol. 32, pp. 1129-1136.

Chang, S., Jain, C., Chuang, T., Feng, L. and Tsao, L. (2011), "Effect of addition of TiO_2 nanoparticles on the microstructure, microhardness and interfacial reactions of Sn3.5AgXCu solder", *Materials & Design*, Vol. 32, pp. 4720-4727.

Che, F., Zhu, W., Poh, E.S., Zhang, X. and Zhang, X. (2010), "The study of mechanical properties of Sn–Ag–Cu lead-free solders with different Ag contents and Ni doping under different strain rates and temperatures", *Journal of Alloys and Compounds*, Vol. 507 No. 1, pp. 215-224.

Chen, B. and Li, G. (2004), "Influence of Sb on IMC growth in Sn–Ag–Cu–Sb Pb-free solder joints in reflow process", *Thin Solid Films*, Vol. 462, pp. 395-401.

Chen, W., Kong, J. and Chen, W. (2011), "Effect of rare earth Ce on the microstructure, physical properties and thermal stability of a new lead-free solder", *Journal of Mining and Metallurgy, Section B: Metallurgy*, Vol. 47 No. 1, pp. 11-21.

Cheng, S., Huang, C.-M. and Pecht, M. (2017), "A review of lead-free solders for electronics applications", *Microelectronics Reliability*, Vol. 75, pp. 77-95.

Chuang, C., Tsao, L., Lin, H. and Feng, L. (2012), "Effects of small amount of active Ti element additions on microstructure and property of Sn3.5Ag0.5Cu solder", *Materials Science and Engineering: A*, Vol. 558, pp. 478-484.

Dharma, I.G.B.B., Shukor, M.H.A. and Ariga, T. (2009), "Wettability of low silver content lead-free solder alloy", *Materials Transactions*, Vol. 50 No. 5, pp. 1135-1138.

Dudek, M. and Chawla, N. (2010), "Effect of rare-earth (La, Ce, and Y) additions on the microstructure and mechanical behavior of Sn-3.9Ag-0.7Cu solder alloy", *Metallurgical and Materials Transactions A*, Vol. 41 No. 3, pp. 610-620.

Efzan Mhd Noor, E., Singh, A. and Tze Chuan, Y. (2013), "A review: influence of nano particles reinforced on solder alloy", *Soldering & Surface Mount Technology*, Vol. 25, pp. 229-241.

Efzan, E. and Marini, A. (2012), "A review of solder evolution in electronic application", *International Journal of Engineering*, Vol. 1, pp. 2305-8269.

El-Daly, A. and El-Taher, A. (2013), "Improved strength of Ni and Zn-doped Sn–2.0Ag–0.5Cu lead-free solder alloys under controlled processing parameters", *Materials & Design*, Vol. 47, pp. 607-614.

El-Daly, A. and Hammad, A. (2012), "Enhancement of creep resistance and thermal behavior of eutectic Sn–Cu lead-free solder alloy by Ag and in-additions", *Materials & Design*, Vol. 40, pp. 292-298.

El-Daly, A., Hammad, A., Fawzy, A. and Nasrallh, D. (2013), "Microstructure, mechanical properties, and deformation behavior of Sn–1.0Ag–0.5Cu solder after Ni and Sb additions", *Materials & Design*, Vol. 43, pp. 40-49.

Fallahi, H., Nurulakmal, M., Arezodar, A.F. and Abdullah, J. (2012), "Effect of iron and indium on IMC formation and mechanical properties of lead-free solder", *Materials Science and Engineering: A*, Vol. 553, pp. 22-31.

Gain, A.K. and Zhang, L. (2018), "The effects of TiO_2 nanoparticles addition on the thermal shock resistance, shear strength and IMC layer growth of SAC305 alloy", *Materialia*, Vol. 3, pp. 64-73.

Gain, A.K. and Zhang, L. (2019), "Effects of Ni nanoparticles addition on the microstructure, electrical and mechanical properties of Sn-Ag-Cu alloy", *Materialia*, Vol. 5, p. 100234.

Gain, A.K., Chan, Y.C. and Yung, W.K. (2011), "Microstructure, thermal analysis and hardness of a Sn–Ag–Cu–1wt% nano-TiO_2 composite solder on flexible ball grid array substrates", *Microelectronics Reliability*, Vol. 51 No. 5, pp. 975-984.

Gain, A.K., Fouzder, T., Chan, Y.C., Sharif, A., Wong, N.B. and Yung, W.K. (2010), "The influence of addition of Al

nano-particles on the microstructure and shear strength of eutectic Sn–Ag–Cu solder on Au/Ni metallized Cu pads", *Journal of Alloys and Compounds*, Vol. 506 No. 1, pp. 216-223.

Gao, L., Xue, S., Zhang, L., Sheng, Z., Zeng, G. and Ji, F. (2010a), "Effects of trace rare earth Nd addition on microstructure and properties of SnAgCu solder", *Journal of Materials Science: Materials in Electronics*, Vol. 21, pp. 643-648.

Gao, L., Xue, S., Zhang, L., Xiao, Z., Dai, W., Ji, F., Ye, H. and Zeng, G. (2010b), "Effect of praseodymium on the microstructure and properties of Sn3.8Ag0.7Cu solder", *Journal of Materials Science: Materials in Electronics*, Vol. 21, pp. 910-916.

Hammad, A. (2013), "Evolution of microstructure, thermal and creep properties of Ni-doped Sn–0.5Ag–0.7Cu low-Ag solder alloys for electronic applications", *Materials & Design (1980-2015)*, Vol. 52, pp. 663-670.

Hammad, A. (2018), "Enhancing the ductility and mechanical behavior of Sn-1.0Ag-0.5Cu lead-free solder by adding trace amount of elements Ni and Sb", *Microelectronics Reliability*, Vol. 87, pp. 133-141.

Hao, H., Tian, J., Shi, Y., Lei, Y. and Xia, Z. (2007), "Properties of Sn3.8Ag0.7Cu solder alloy with trace rare earth element Y additions", *Journal of Electronic Materials*, Vol. 36 No. 7, pp. 766-774.

Harrison, M., Vincent, J. and Steen, H. (2001), "Lead-free reflow soldering for electronics assembly", *Soldering & Surface Mount Technology*, Vol. 13, pp. 21-38.

Haseeb, A. and Leng, T.S. (2011), "Effects of Co nanoparticle addition to Sn–3.8Ag–0.7Cu solder on interfacial structure after reflow and ageing", *Intermetallics*, Vol. 19 No. 5, pp. 707-712.

Haseeb, A., Arafat, M., Tay, S. and Leong, Y. (2017), "Effects of metallic nanoparticles on interfacial intermetallic compounds in tin-based solders for microelectronic packaging", *Journal of Electronic Materials*, Vol. 46 No. 10, pp. 5503-5518.

Huang, M. and Wang, L. (2005), "Effects of Cu, Bi, and in on microstructure and tensile properties of Sn-Ag-X (Cu, Bi, in) solders", *Metallurgical and Materials Transactions A*, Vol. 36 No. 6, pp. 1439-1446.

Jeon, S-J., Hyun, S., Lee, H.-J., Kim, J.-W., Ha, S.-S., Yoon, J.-W., Jung, S.-B. and Lee, H.-J. (2008), "Mechanical reliability evaluation of Sn-37Pb solder joint using high speed lap-shear test", *Microelectronic Engineering*, Vol. 85 No. 10, pp. 1967-1970.

Jung, D.-H., Sharma, A. and Jung, J.-P. (2018), "Influence of dual ceramic nanomaterials on the solderability and interfacial reactions between lead-free Sn-Ag-Cu and a Cu conductor", *Journal of Alloys and Compounds*, Vol. 743, pp. 300-313.

Kanlayasiri, K. and Meesathien, N. (2018), "Effects of zinc oxide nanoparticles on properties of SAC0307 lead-free solder paste", *Advances in Materials Science and Engineering*, Vol. 2018, pp. 1-10.

Kanlayasiri, K., Mongkolwongrojn, M. and Ariga, T. (2009), "Influence of indium addition on characteristics of Sn–0.3Ag–0.7Cu solder alloy", *Journal of Alloys and Compounds*, Vol. 485 Nos 1/2, pp. 225-230.

Kumar, K.M., Kripesh, V. and Tay, A.A. (2008), "Single-wall carbon nanotube (SWCNT) functionalized Sn–Ag–Cu lead-free composite solders", *Journal of Alloys and Compounds*, Vol. 450 Nos 1/2, pp. 229-237.

Lee, N.-C. (1997), "Getting ready for lead-free solders", *Soldering & Surface Mount Technology*, Vol. 9, pp. 65-69.

Leong, Y. and Haseeb, A. (2016), "Soldering characteristics and mechanical properties of Sn-1.0Ag-0.5Cu solder with minor aluminum addition", *Materials*, Vol. 9 No. 7, p. 522.

Li, G., Chen, B., Shi, X., Wong, S.C. and Wang, Z. (2006), "Effects of Sb addition on tensile strength of Sn–3.5Ag–0.7Cu solder alloy and joint", *Thin Solid Films*, Vol. 504 Nos 1/2, pp. 421-425.

Li, Y., Zhao, X., Liu, Y., Wang, Y. and Wang, Y. (2014), "Effect of TiO_2 addition concentration on the wettability and intermetallic compounds growth of Sn3.0Ag0.5Cu–xTiO_2 nano-composite solders", *Journal of Materials Science: Materials in Electronics*, Vol. 25, pp. 3816-3827.

Liang, J., Luo, T., Hu, A. and Li, M. (2014), "Formation and growth of interfacial intermetallic layers of Sn–8Zn–3Bi–0.3Cr on Cu, Ni and Ni–W substrates", *Microelectronics Reliability*, Vol. 54 No. 1, pp. 245-251.

Liu, P., Yao, P. and Liu, J. (2008), "Effect of SiC nanoparticle additions on microstructure and microhardness of Sn-Ag-Cu solder alloy", *Journal of Electronic Materials*, Vol. 37 No. 6, pp. 874-879.

Liu, X., Han, Y., Jing, H., Wei, J. and Xu, L. (2013), "Effect of graphene nanosheets reinforcement on the performance of SnAgCu lead-free solder", *Materials Science and Engineering: A*, Vol. 562, pp. 25-32.

Luo, D-X., Xue, S-B. and Li, Z-Q. (2014), "Effects of Ga addition on microstructure and properties of Sn–0.5 Ag–0.7 Cu solder", *Journal of Materials Science: Materials in Electronics*, Vol. 25, pp. 3566-3571.

Ma, H. and Suhling, J.C. (2009), "A review of mechanical properties of lead-free solders for electronic packaging", *Journal of Materials Science*, Vol. 44 No. 5, pp. 1141-1158.

Mei, Z., Holder, H.A. and Vander Plas, H.A. (1996), "Low-temperature solders", *Hewlett Packard Journal*, Vol. 47, pp. 91-98.

Nai, S., Wei, J. and Gupta, M. (2006), "Influence of ceramic reinforcements on the wettability and mechanical properties of novel lead-free solder composites", *Thin Solid Films*, Vol. 504 Nos 1/2, pp. 401-404.

Nai, S., Wei, J. and Gupta, M. (2008), "Effect of carbon nanotubes on the shear strength and electrical resistivity of a lead-free solder", *Journal of Electronic Materials*, Vol. 37 No. 4, pp. 515-522.

Nimmo, K. (2004), "Alloy selections", *Lead-Free Soldering in Electronics – Science, Technology and Environmental Impact*, pp. 49-90.

Roshanghias, A., Kokabi, A., Miyashita, Y., Mutoh, Y., Rezayat, M. and Madaah-Hosseini, H. (2012), "Ceria reinforced nanocomposite solder foils fabricated by accumulative roll bonding process", *Journal of Materials Science: Materials in Electronics*, Vol. 23, pp. 1698-1704.

Sabri, M.F.M., Shnawah, D.A., Badruddin, I.A., Said, S.B. M., Che, F.X. and Ariga, T. (2013), "Microstructural stability of Sn–1Ag–0.5 Cu–xAl (x= 1, 1.5, and 2wt.%) solder alloys and the effects of high-temperature aging on

their mechanical properties", *Materials Characterization*, Vol. 78, pp. 129-143.

Sadiq, M. (2012), "Design and fabrication of lanthanum-doped Sn-Ag-Cu lead-free solder for next generation microelectronics applications in severe environment", Doctoral dissertation, Georgia Institute of Technology.

Sadiq, M., Pesci, R. and Cherkaoui, M. (2013), "Impact of thermal aging on the microstructure evolution and mechanical properties of lanthanum-doped tin-silver-copperlead-free solders", *Journal of Electronic Materials*, Vol. 42 No. 3, pp. 492-501.

Sharma, A., Yu, H., Cho, I.S., Seo, H. and Ahn, B. (2019), "ZrO_2 nanoparticle embedded low silver lead free solder alloy for modern electronic devices", *Electronic Materials Letters*, Vol. 15 No. 1, pp. 27-35.

Shi, Y., Tian, J., Hao, H., Xia, Z., Lei, Y. and Guo, F. (2008), "Effects of small amount addition of rare earth Er on microstructure and property of SnAgCu solder", *Journal of Alloys and Compounds*, Vol. 453 Nos 1/2, pp. 180-184.

Shnawah, D.A., Sabri, M.F.M. and Badruddin, I.A. (2012), "A review on thermal cycling and drop impact reliability of SAC solder joint in portable electronic products", *Microelectronics Reliability*, Vol. 52 No. 1, pp. 90-99.

Shnawah, D.A., Sabri, M.F.M., Badruddin, I.A., Said, S.B. M., Ariga, T. and Che, F.X. (2013), "Effect of Ag content and the minor alloying element Fe on the mechanical properties and microstructural stability of Sn-Ag-Cu solder alloy under high-temperature annealing", *Journal of Electronic Materials*, Vol. 42 No. 3, pp. 470-484.

Sona, M. and Prabhu, K. (2013), "Review on microstructure evolution in Sn–Ag–Cu solders and its effect on mechanical integrity of solder joints", *Journal of Materials Science: Materials in Electronics*, Vol. 24, pp. 3149-3169.

Sujan, G., Haseeb, A., Nishikawa, H. and Amalina, M. (2017), "Interfacial reaction, ball shear strength and fracture surface analysis of lead-free solder joints prepared using cobalt nanoparticle doped flux", *Journal of Alloys and Compounds*, Vol. 695, pp. 981-990.

Sun, L. and Zhang, L. (2015), "Properties and microstructures of Sn-Ag-Cu-X lead-free solder joints in electronic packaging", *Advances in Materials Science and Engineering*, Vol. 2015, p. 16.

Tang, Y., Li, G. and Pan, Y. (2014), "Effects of TiO_2 nanoparticles addition on microstructure, microhardness and tensile properties of Sn–3.0Ag–0.5Cu–xTiO_2 composite solder", *Materials & Design*, Vol. 55, pp. 574-582.

Tay, S., Haseeb, A., Johan, M.R., Munroe, P. and Quadir, M. Z. (2013), "Influence of Ni nanoparticle on the morphology and growth of interfacial intermetallic compounds between Sn–3.8Ag–0.7Cu lead-free solder and copper substrate", *Intermetallics*, Vol. 33, pp. 8-15.

Tsao, L., Chang, S., Lee, C., Sun, W. and Huang, C. (2010), "Effects of nano-Al_2O_3 additions on microstructure development and hardness of Sn3.5Ag0.5Cu solder", *Materials & Design*, Vol. 31, pp. 4831-4835.

Tsao, L., Wu, R., Cheng, T.-H., Fan, K.-H. and Chen, R. (2013), "Effects of nano-Al_2O_3 particles on microstructure and mechanical properties of Sn3.5Ag0.5Cu composite solder ball grid array joints on Sn/Cu pads", *Materials & Design*, Vol. 50, pp. 774-781.

Tu, X., Yi, D., Wu, J. and Wang, B. (2017), "Influence of Ce addition on Sn-3.0Ag-0.5Cu solder joints: thermal behavior, microstructure and mechanical properties", *Journal of Alloys and Compounds*, Vol. 698, pp. 317-328.

Vianco, P. and Shangguan, D. (2006), *Fatigue and Creep of Lead-Free Solder Alloys: fundamental Properties, Chapter 3, Leadfree Solder Interconnect Reliability*, ASM International, Materials Park, OH, pp. 67-106.

Wang, H., Lu, T., Yi, D. and Wang, B. (2019), "Microstructure refinement, characterization of tensile behavior and aging resistance of Zr-modified SAC105 solder alloy", *Journal of Materials Science: Materials in Electronics*, Vol. 30, pp. 11429-11439.

Wang, J.-X., Xue, S.-B., Han, Z.-J., Yu, S.-L., Chen, Y., Shi, Y.-P. and Wang, H. (2009), "Effects of rare earth Ce on microstructures, solderability of Sn–Ag–Cu and Sn–Cu–Ni solders as well as mechanical properties of soldered joints", *Journal of Alloys and Compounds*, Vol. 467 Nos 1/2, pp. 219-226.

Wu, C. and Wong, Y. (2007), "Rare-earth additions to lead-free electronic solders", *Journal of Materials Science: Materials in Electronics*, Vol. 18, pp. 77-91.

Wu, C., Yu, D., Law, C. and Wang, L. (2004), "Properties of lead-free solder alloys with rare earth element additions", *Materials Science and Engineering: R: Reports*, Vol. 44 No. 1, pp. 1-44.

Xia, Z., Chen, Z., Shi, Y., Mu, N. and Sun, N. (2002), "Effect of rare earth element additions on the microstructure and mechanical properties of tin-silver-bismuth solder", *Journal of Electronic Materials*, Vol. 31 No. 6, pp. 564-567.

Xiong, M-y. and Zhang, L. (2019), "Interface reaction and intermetallic compound growth behavior of Sn-Ag-Cu lead-free solder joints on different substrates in electronic packaging", *Journal of Materials Science*, Vol. 54 No. 2, pp. 1741-1768.

Xu, L., Wang, L., Jing, H., Liu, X., Wei, J. and Han, Y. (2015), "Effects of graphene nanosheets on interfacial reaction of Sn–Ag–Cu solder joints", *Journal of Alloys and Compounds*, Vol. 650, pp. 475-481.

Yakymovych, A., Plevachuk, Y., Sklyarchuk, V., Sokoliuk, B., Galya, T. and Ipser, H. (2017), "Microstructure and electro-physical properties of Sn-3.0Ag-0.5Cu nanocomposite solder reinforced with Ni nanoparticles in the melting-solidification temperature range", *Journal of Phase Equilibria and Diffusion*, Vol. 38 No. 3, pp. 217-222.

Yang, Z., Zhou, W. and Wu, P. (2014), "Effects of Ni-coated carbon nanotubes addition on the microstructure and mechanical properties of Sn–Ag–Cu solder alloys", *Materials Science and Engineering: A*, Vol. 590, pp. 295-300.

Yasmin, T. and Sadiq, M. (2014), "Impact of lanthanum doping on SAC305 lead free solders for high temperature applications", *Journal of Engineering and Applied Sciences (JEAS)*, Vol. 33 No. 1, pp. 29-36.

Yoon, J.-W., Kim, S.-W. and Jung, S.-B. (2005), "IMC morphology, interfacial reaction and joint reliability of Pb-free Sn–Ag–Cu solder on electrolytic Ni BGA substrate", *Journal of Alloys and Compounds*, Vol. 392 Nos 1/2, pp. 247-252.

Zhang, L., Fan, X-y., Guo, Y-h. and He, C-W. (2014), "Properties enhancement of SnAgCu solders containing rare earth Yb", *Materials & Design*, Vol. 57, pp. 646-651.

Zhang, L., Han, J-G., He, C-W. and Guo, Y-h. (2012a), "Effect of Zn on properties and microstructure of SnAgCu alloy", *Journal of Materials Science: Materials in Electronics*, Vol. 23, pp. 1950-1956.

Zhang, L., Xue, S.B., Zeng, G., Gao, L.L. and Ye, H. (2012b), "Interface reaction between SnAgCu/SnAgCuCe solders and Cu substrate subjected to thermal cycling and isothermal aging", *Journal of Alloys and Compounds*, Vol. 510 No. 1, pp. 38-45.

Zhu, Z., Chan, Y.-C., Chen, Z., Gan, C.-L. and Wu, F. (2018), "Effect of the size of carbon nanotubes (CNTs) on the microstructure and mechanical strength of CNTs-doped composite Sn0.3Ag0.7Cu-CNTs solder", *Materials Science and Engineering: A*, Vol. 727, pp. 160-169.

Corresponding author

Muhammad Aamir can be contacted at: m.aamir@ecu.edu.au